Teleoperation control based on combination of wave variable and neural networks

Article (Accepted Version)

Teleoperation Control based on Combination of Wave Variable and Neural Networks

Chenguang Yang, Xingjian Wang, Zhijun Li, Yanan Li, Chun-Yi Su

***Abstract*—In this paper, a novel control scheme is developed for a teleoperation system, combining the radial basis function (RBF) neural networks (NNs) and wave variable technique to simultaneously compensate for the effects caused by communication delays and dynamics uncertainties. The teleoperation system is set up with a TouchX joystick as the master device and a simulated Baxter robot arm as the slave robot. The haptic feedback is provided to the human operator to sense the interaction force between the slave robot and the environment when manipulating the stylus of the joystick. To utilize the workspace of the telerobot as much as possible, a matching process is carried out between the master and the slave based on their kinematics models. The closed loop inverse kinematics (CLIK) method and RBF NN approximation technique are seamlessly integrated in the control design. To overcome the potential instability problem in the presence of delayed communication channels, wave variables and their corrections are effectively embedded into the control system, and Lyapunov based analysis is performed to theoretically establish the closed-loop stability. Comparative experiments have been conducted for a trajectory tracking task, under the different conditions of various communication delays. Experimental results show that in terms of tracking performance and force reflection, the proposed control approach shows superior performance over the conventional methods.**

***Index Terms*—Neural Networks; Teleoperation Control; Wave Variable; Time-Varying Delay**

I. INTRODUCTION

In the past decades, robotic technologies have been developed rapidly in a wide range of engineering fields. The telerobot operation as one of the most attractive and challenging topic in robotics has been used in various applications such as telesurgery, search and rescue, 3D game development and so on [1]. A typical teleoperation system usually comprises 5 parts: human operator, master device, communication channels, slave robot and environment [2]. Usually, the human operator controls the motion of a master device, which is physically in contact with human. The master device generates commanding trajectories passed through the communication channels, which are passed to the slave robot that acts on the target environment and completes the task. The interaction force between the slave robot and the environment is fedback to the master, according to which the human operator could control the robot more effectively.

In this paper, we use a Geomagic® TouchX as the master device, which is designed by the SensAble Technologies Inc. TouchX is a haptic feedback device including both hardware drives and software packages (OpenHaptics® toolkit) [1]. The TouchX arm includes 3 rotational joints, each joint is equipped with a motor to generate the feedback force. A 3 degrees of freedom (DOFs) gimbal joint stylus is installed at the end of the manipulator to provide the orientation motion. As a slave robot, there are 7 revolute joints in each arm of Baxter, which make it easy to move in the 3-D space [3]. In order to grasp and handle the objects, a rotational gripper is installed at the end-effector of each arm. The MATLAB Robotics Toolbox [4] is used to establish the kinematics and dynamics models of the Baxter robot arm, which is used as the slave telerobot to test the proposed method.

As we known, the communication channels play significant roles in a teleoperation systems, and time delays in the channels may cause system unstable in the presence of force feedback [5]. Much effort has been made to handle the effect of time delays [6], especially in the bilateral teleoperation system [7], [8]. The notion of wave variable was proposed and it has been established in [9] that the wave variable could guarantee the stability of the communication with time delays. The influence of time-varying delays to the stability of a teleoperation system was studied in [10]. In [2], the method of integrating the corrected wave was investigated to remove the distortion caused by the transmission of wave variables. A wave variable based control was proposed in [11] to handle the problem in the bilateral time-varying system. Based on this idea, a novel approach was presented for controlling the time-varying delayed teleoperation system with a PD controller [12].

Due to the existence of uncertainties in practical application-

This work was partially supported by National Nature Science Foundation (NSFC) under Grants 61473120, 61573147 and 91520201, Guangdong Provincial Natural Science Foundation 2014A030313266 and International Science and Technology Collaboration Grant 2015A050502017, Science and Technology Planning Project of Guangzhou 201607010006 and the Fundamental Research Funds for the Central Universities under Grant 2015ZM065.

C. Yang, X. Wang, Z. Li and C.-Y. Su are with Key Laboratory of Autonomous Systems and Networked Control, College of Automation Science and Engineering, South China University of Technology, Guangzhou, 510640 China. (Email: cyang@ieee.org; xj.wang_scut@qq.com; zjli@ieee.org;chunyi.su@concordia.ca). C. Yang is also with Zienkiewicz Centre for Computational Engineering, Swansea University, SA1 8EN, UK. C.-Y. Su is on leave from Concordia University, Canada.

Y. Li is with Department of Bioengineering, Imperial College London, SW7 2AZ London, UK. (Email: yanan.li@imperial.ac.uk)

s [13], the research on controlling the uncertain robot system becomes significantly important. The adaptive control method for robots has been studied in a considerable number of works [14]–[16], which could be used in the situations of unknown parameters and time-varying parameters in the robot model [17], [18]. Time-varying delays and uncertainties of the robot model have been studied together with adaptive control in [19], [20]. In [21]–[23], adaptive fuzzy control was used for identification of the unknown nonlinear control system. Fuzzy control was used for studying uncertain nonlinear systems in [24], [25]. In [26], fuzzy control was adopted to improve the performance of the automobile cruise system. In recent years, the applications of NN to the robot control system have become increasingly popular [27]–[31], due to the fact that the NN has the ability to emulate complicated nonlinearity and uncertain functions [32]–[34]. The RBF NN is a highly effective method and has been extensively used for control design of uncertain robot systems [35]. Adaptive RBF NN based control has been investigated in [36], [37] to deal with the deadzone and uncertain robotic model. In [38], an adaptive NN method was applied to achieve control of the uncertain marine vessel system. In [39], a controller was designed for dual-arm coordination of a humanoid robot based on the adaptive neural control. The tracking performance of the adaptive NN control for a discrete-time system was studied in [40]. In [41], the effectiveness of the NN control was firstly considered in the Prandtl-Ishlinskii (PI) hysteresis system. The RBF NN was investigated in [42] as a compensator to solve the non-linearities problem that a standard PD controller could not handle. In [43], the RBF NN was used to learn the robot behavior, and in [44] the RBF NN was investigated to improve the behaviour of the non-linear actuator. In [45], trajectory control of a fruit and vegetable picking robot was studied, and in [46] the RBF NN was used to compensate for the deadzone of the non-linear system. In [47], the RBF NN has been discussed in detail for compensation for the tracking error in controlling mobile robots. In this paper, a NN controller based on the PD control is applied to the slave robot with 7 DOFs, which guarantees more accurate trajectory tracking than the conventional PD controller.

The reminder of the paper is organized as follows: in Section II, the computational model of the master-slave teleoperation system is analysed. In Section III, the PD control on the master and slave is first discussed, and the nonlinear uncertainties of the model of the slave robot are then analysed. The CLIK method is used for avoiding kinematic singularities and numerical drifts. The RBF NN control is designed for the slave robot. Finally, the convergence of the tracking error and the stability of the teleoperation system with the time-varying delays are established. Comparative experiments are carried out in Section IV and conclusions and possible future work are discussed in Section V.

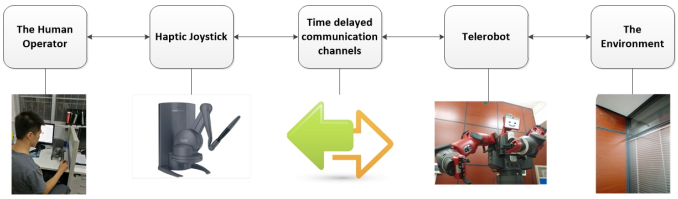

Fig. 1. The system framework

Throughout this paper, the following notions are used

- $0_{m\times n}$ stands for an $m \times n$ dimensional zero matrix.
- $\|\cdot\|$ denotes the Euclidean norm of vectors and induced norm of matrices.
- $A := B$ means that B is defined as A.
- sup means the least upper bound of a partially ordered set.
- $\lambda(\cdot)$ stands for eigenvalue of a matrix.
- $\Re(\cdot)$ stands for real part of a complex number.
- L_2 is a function space and the functions in L_2 are quadratically integrable. L_∞ is a function space and the functions in L_∞ are essentially bounded measurable.
- tr stands for trace of a matrix.

II. MATHEMATICAL MODEL OF TELEOPERATION SYSTEM

A. Illustration of Teleoperation System

The teleoperation system in this paper is shown in Fig. 1. As we see, the human operator holds the stylus of the haptic device and drives the motion of the master device, which will be regarded as position commands. Through processing by the master computer, the new commands will be generated by the master computer and then passed to the slave computer and received by the slave controller. The Baxter robot will move in accordance with the commands from the slave controller. The manipulator end-effector interacts with the environment, and the interaction force is passed to the haptic device to be sensed by the human operator, which will lead to a new movement and new control commands. In next five subsections we will analyze the mathematical models of the components of the teleoperation system.

B. Kinematics and Dynamics of Master Robot Arm

The haptic device Geomagic TouchX not only sends commands of movement to the master device, but also returns the interaction force between the telerobot and the environment, and this is very useful for the operator to regulate the contact force [48]. The mathematical model of the master includes the kinematics model and the dynamics model.

The kinematics model of TouchX is built based on its structure, as shown in Fig. 2. With 6 revolute joints, three of them are equipped with motors, and the other three are gimbal joint stylus considered as an end-effector, making it flexible to move within the workspace. For more concrete and

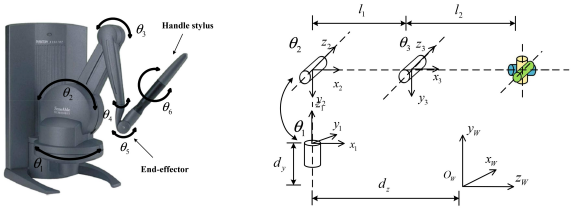

Fig. 2. The structure of TouchX

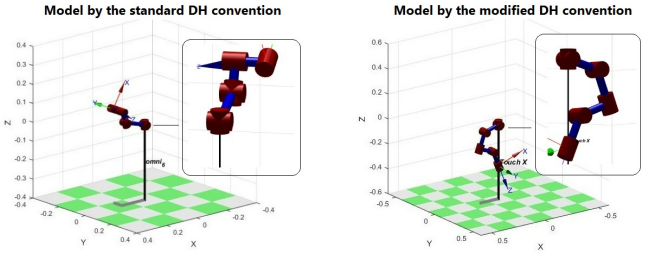

Fig. 3. Comparison between two kinematics models of TouchX based on standard DH parameters and modified DH parameters

intuitive representation of its structure, the Denavit Hartenburg (DH) parameters are used to build the kinematics model [3].

There are two representations for DH parameters, the standard DH convention [49] and the modified DH convention [50], and the latter representation is used for the kinematics modelling of the TouchX joystick in this work. According to the standard DH convention, the origins of the coordinates relevant to joint 4 and joint 5 as shown in the left panel of Fig. 3 are the same. Consequently, the simulated robot modeled by the MATLAB Robotics Toolbox should be modified. Specifically, a_{i-1} and d_i are used to represent the link length and the link offset, respectively, where i represents the ith joint of the master device. α_{i-1} and θ_i are used to represent the joint twist angle and joint angle, respectively. All the 6 joints of the master device are revolute, and the modified DH parameters of the TouchX are obtained in Tab. I.

The DH parameters in Tab. I represent the structure characteristics of the master device, from which the kinematics model could be obtained. According to [3], the homogeneous transformation between two adjacent coordinates in Fig. 1

TABLE I
DH PARAMETERS (MODIFIED CONVENTION) OF THE MASTER DEVICE

Link i	θ_i (angle limit(deg))	d_i	a_{i-1}	α_{i-1}(rad)
1	q_1(-60∼60)	0	0	0
2	q_2(0∼105)	0	0	$-\pi/2$
3	q_3(-180∼180)	0	L_{m1}	0
4	q_4(-145∼145)	L_{m2}	0	$-\pi/2$
5	q_5(-70∼70)	0	0	$-\pi/2$
6	q_6(-145∼145)	0	0	$-\pi/2$

could be formulated using DH parameters as follows:

$$ {}^{i-1}A_i(\theta_i, d_i, a_i, \alpha_i) = \begin{bmatrix} c\theta_i & -s\theta_i c\alpha_i & s\theta_i c\alpha_i & a_i c\theta_i \\ c\theta_i & c\theta_i c\alpha_i & -c\theta_i c\alpha_i & a_i s\theta_i \\ 0 & s\alpha_i & c\alpha_i & d_i \\ 0 & 0 & 0 & 1 \end{bmatrix} \tag{1} $$

where "c" is short for trigonometric function "$\cos$" and "s" is short for "$\sin$".

Moreover, the relationship between the position of the end effector and the base could be calculated as follows:

$$ {}^{n}X_0 = {}^{0}A_1 {}^{1}A_2 ... {}^{n-1}A_n \cdot X_n \tag{2} $$

where n is 6 for the master device, $X = [x, y, z, 1]$ represents the position of the related joint, and ${}^{i}A_{i+1} (i = 0, 1, ..., n-1)$ represents the adjacent coordinate in (1).

The dynamics model of the master device reveals the relationship between the driving torque or related force and joint motion, and could be represented as follows:

$$ M_m(q_m)\ddot{q}_m + h_m(q_m, \dot{q}_m) = J_m^T F_h - \tau_m + f_m \tag{3} $$

where

$$ h_m(q_m, \dot{q}_m) = C_m(q_m, \dot{q}_m)\dot{q}_m + G_m(q_m) \tag{4} $$

with the subscript "m" used to indicate master. For a robot manipulator with n-DOF serial links and all the joints revolute, q_m, $\dot{q}_m$ and $\ddot{q}_m \in \mathbb{R}^n$ are the joint position, velocity and acceleration, respectively. $M_m(q_m)\ddot{q}_m \in \mathbb{R}^{n\times n}$ is the inertia matrix. $h_m(q_m, \dot{q}_m)$ represents the nonlinear coupling term of the centripetal force, Coriolis force and the gravity force. f_m represents coulomb friction, load changes, time-delayed jamming and other disturbances. J_m is the Jacobian matrix and J_m^T is its transpose. F_h is the force exerted by the human operator and τ_m is the torque control signal, both of which will be applied to the master device. The terms on the left hand side of Eqs. (3) and (4) satisfy the following properties [51]:

Property 1: The matrix $M_m(q_m) \in \mathbb{R}^{n\times n}$ is a symmetric positive-definite matrix.

Property 2: The matrix $\dot{M}_m(q_m) - 2C_m(q_m, \dot{q}_m)$ is a skew-symmetric matrix, i.e., $z^T\left(\dot{M}_m - 2C_m\right)z = 0,\ \forall z \in R^n$.

Property 3: $M_m(q_m)$ and $G_m(q_m)$ are bounded, and $C_m(q_m, \dot{q}_m)$ satisfies that $\forall q_m, \dot{q}_m \in \mathbb{R}^n, \exists K_{cm} \in \mathbb{R}_{>0}$ such that $\|C_m(q_m, \dot{q}_m)\| \leq K_{cm}|\dot{q}_m|^2$.

C. Model of the Slave Robot

Fig. 4 shows the structure of the Baxter robot, which is a dual-arm robot with 7-DOFs per arm. In this paper, the simulated left arm of the Baxter robot is taken as the slave telerobot.

The standard DH parameters are used to describe the structure of the left arm of the Baxter robot, as shown in Tab. II. The lengths mentioned in Fig. 4 and Tab. II are L_{s0} = 0.27m, L_{s1} = 0.069m, L_{s2} = 0.364m, L_{s3} = 0.069m, L_{s4}

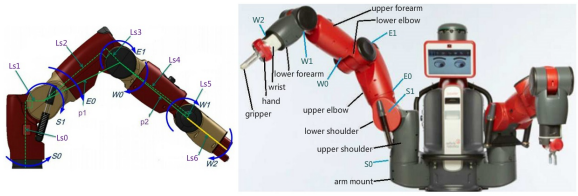

Fig. 4. The structure of the Baxter robot

TABLE II
DH PARAMETERS (STANDARD CONVENTION) OF THE SLAVE ROBOT

Link i	θ_i (anglelimit(deg))	d_i	a_i	α_i(rad)
1	q_1(-97.5∼97.5)	L_{s0}	L_{s1}	$-\pi/2$
2	$q_2 + \frac{\pi}{2}$(-123∼60)	0	0	$\pi/2$
3	q_3(-175 ∼ 175)	L_{s2}	L_{s3}	$-\pi/2$
4	q_4(2.865 ∼ 150)	0	0	$\pi/2$
5	q_5(-175.27 ∼ 175.27)	L_{s4}	L_{s5}	$-\pi/2$
6	q_6(-90 ∼ 120)	0	0	$\pi/2$
7	q_7(-175.27 ∼ 175.27)	L_{s6}	0	0

= 0.375m, L_{s5} = 0.01m and L_{s6} = 0.28m. According to Eqs. (1) and (2), the forward kinematics model of the Baxter robot could be obtained, and n used in (2) is 7.

In order to achieve a precise tracking of the position commanded by the master joystick, a workspace matching between the master joystick and the slave telerobot is essential. The Monte Carlo method used in [3] was applied to approximate the workspace for the master and the slave. In order to make sure that the transformed workspace of the master device is constrained within that of the slave robot, the workspace of the master is scaled in a fixed proportion [52]. Fig. 5 shows the workspace of the master and that of the slave after the matching process. The top left panel of Fig. 5 shows the enveloped surface, generated as convex hull of the 3D clouds of the workspaces of both master and slave after the matching process. Similar to the workspace transformation developed in [3] between the Baxter robot arm and the Omni joystick, in this work, the workspace transformation between the Baxter robot arm and the TouchX joystick is given as below:

$$\begin{bmatrix} x_s \\ y_s \\ z_s \end{bmatrix} = \begin{bmatrix} cos\delta & -sin\delta & 0 \\ sin\delta & cos\delta & 0 \\ 0 & 0 & 1 \end{bmatrix} \times \left(\begin{bmatrix} S_x & 0 & 0 \\ 0 & S_y & 0 \\ 0 & 0 & S_z \end{bmatrix} \begin{bmatrix} x_m \\ y_m \\ z_m \end{bmatrix} + \begin{bmatrix} T_x \\ T_y \\ T_z \end{bmatrix} \right) \tag{5}$$

where $[x_s, y_s, z_s]^T$, $[x_m, y_m, z_m]^T$ represent the Cartesian coordinates of the end-effectors of Baxter and TouchX joystick, respectively. δ is the rotation angle of Z axis for the base of the master device, $[S_x, S_y, S_z]^T$ and $[T_x, T_y, T_z]^T$ are the proportionality factors and offset correction terms about the X, Y and Z axes, respectively. According to [3], the matching parameters of (6) are given by

$$\delta = \frac{\pi}{4}, \begin{bmatrix} S_x \\ S_y \\ S_z \end{bmatrix} = \begin{bmatrix} 0.0041 \\ 0.0040 \\ 0.0041 \end{bmatrix}, \begin{bmatrix} T_x \\ T_y \\ T_z \end{bmatrix} = \begin{bmatrix} 0.701 \\ 0.210 \\ 0.129 \end{bmatrix}$$

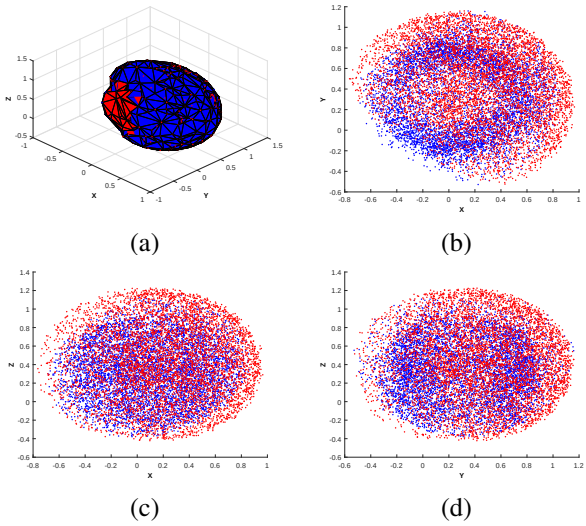

Fig. 5. Workspace matching. (a) The 3-D envelope surface of the master and the slave. (b) Workspace matching in the X-Y plane. (c) Workspace matching in the X-Z plane. (d) Workspace matching in the Y-Z plane

The dynamics model of the telerobot could be represented as follows

$$M_s(q_s)\ddot{q}_s + h_s(q_s, \dot{q}_s) = \tau_s - J_s^T F_e + f_s \tag{6}$$

$$h_s(q_s, \dot{q}_s) = C_s(q_s, \dot{q}_s)\dot{q}_s + G_s(q_s) \tag{7}$$

where the subscript "s" is used to indicate slave. The denotations of the components on the left hand side of Eqs. (6) and (7) are similar to those of Eqs. (3) and (4). F_e is the interaction force between the environment and the telerobot, and τ_s is the control input to the slave.

D. Model of the Human Operator

Early studies have shown that the muscle property of the human hand could be modelled as a spring. A more complete mass spring damper model is proposed in [53]. In the teleoperation system, the human hand holds the stylus of the master joystick, and gives the corresponding position and velocity commands. Even if the master device is subjected to the environmental force transmitted from the slave, the operator could also adjust the output of the hand to make the master track the desired movement of the operator. Therefore, the human hand could actually be regarded as controlled by an intelligent proportional-integral (PI) controller, which could adjust the output force of the hand according to the error between the actual position x_m and the desired position x_{md} of the master described by

$$F_h = K_{hp}(x_{md} - x_m) + K_{hi}\int_{t_0}^{t}(x_{md} - x_m)dt \tag{8}$$

where K_{hp} and K_{hi} are the proportional gain and integral gain of the human hand, respectively. The notations of t_0 and t are the initial time instant and the current time instant, respectively.

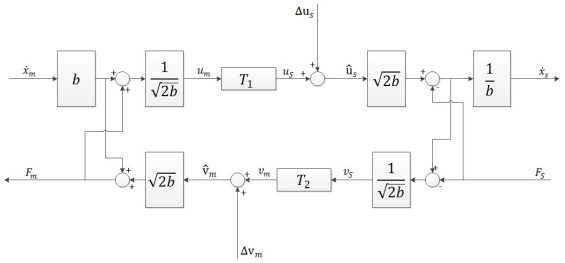

Fig. 6. Communication with wave variables

E. Model of the Environment

In this work, a simple mathematical model of the environment is considered. It describes the relationship between the interaction force of the environment F_e and the slave robot position x_s, i.e.,

$$F_e = K_{sp}(x_s - x_e) + K_{sd}\dot{x}_s \tag{9}$$

where K_{sp} and K_{sd} are the parameters of the environment, and x_e is the position of the environment. In the free space movement, $K_{sp} = K_{sd} = 0_{m\times n}$.

F. Model of the Communication Channels

The wave variable approach for the time-varying delayed communication is used in this section. In the teleoperation system shown in Fig. 6, the velocity $\dot{x}$ and the force F of both master and slave flow into the communication channels, and are then transformed into the power variables u and v as follows

$$u_m = (b\dot{x}_m + F_m)/\sqrt{2b}\,, \hat{v}_m = (b\dot{x}_m - F_m)/\sqrt{2b} \tag{10}$$
$$\hat{u}_s = (b\dot{x}_s + F_s)/\sqrt{2b}\,, v_s = (b\dot{x}_s - F_s)/\sqrt{2b} \tag{11}$$

where b is the wave impedance [54].

In the communication channels, the time-varying delays T_1 and T_2 between the wave variables could be represented as follows

$$u_s(t) = u_m(t - T_1(t)) \tag{12}$$
$$v_m(t) = v_s(t - T_2(t)) \tag{13}$$

In Fig. 6, we see that the relationship between the wave variables and the power variables is as follows:

$$\dot{x}_m = (u_m + \hat{v}_m)/\sqrt{2b}\,, F_m = (u_m - \hat{v}_m)/\sqrt{2b} \tag{14}$$
$$\dot{x}_s = (\hat{u}_s + v_s)/\sqrt{2b}\,, F_s = (\hat{u}_s - v_s)/\sqrt{2b} \tag{15}$$

The flowing power in the communication channels could be calculated by the power variables and the wave variables

$$\begin{aligned} P(t) =& \dot{x}_m^T F_m - \dot{x}_s^T F_s \\ =& \frac{1}{2}(u_m^T u_m - v_m^T v_m - u_s^T u_s + v_s^T v_s) \\ =& \frac{1}{2}(u_m^T u_m - u_m^T(t-T_1)u_m(t-T_1) + v_s^T v_s \\ & - v_s^T(t-T_1)v_s(t-T_1)) \\ =& \frac{d}{dt}(\frac{1}{2}\int_{t-T_1}^{t} u_m^T u_m d\sigma + \frac{1}{2}\int_{t-T_2}^{t} v_s^T v_s d\sigma) \end{aligned} \tag{16}$$

Under the condition of time delays, the energy E stored in the communication could be calculated as follows

$$\begin{aligned} E(t) =& \int_0^t \left(\dot{x}_m^T F_m - \dot{x}_s^T F_s\right) d\sigma \\ =& \frac{1}{2}(\int_{t-T_1}^{t} u_m^T u_m d\sigma + \int_{t-T_2}^{t} v_s^T v_s d\sigma) \end{aligned} \tag{17}$$

where time delays T_1 and T_2 are constant and the energy satisfies $E > 0$, such that the system shown in Fig. 6 is passive [9]. When the delays are time varying, the proof for the system passivity is nontrivial and far more complicated than (17). It will be discussed in detail later in Section III.

To handle the time-varying delays in the communication of the teleoperation system, the wave correction method is employed [12], as shown in Fig. 6, which could be represented as follows

$$\hat{u}_s = u_m(t - T_1(t)) + \Delta u_s \tag{18}$$
$$\hat{v}_m = v_s(t - T_2(t)) + \Delta v_m \tag{19}$$

where $\hat{u}_s$ and $\hat{v}_m$ are obtained by using the corrective waves Δu_s and Δv_m represented as below [12]

$$\Delta u_s(t) = \sqrt{2b}\lambda\left[x_{mf}(t) + x_{dh} - x_{sd}(t)\right] \tag{20}$$

$$\Delta v_m(t) = \sqrt{2b}\lambda\left[x_{sf}(t) + x_{dh} - x_{md}(t)\right] \tag{21}$$

where $\lambda > 0$ is designed for the convergence of position. The gravity factor, x_{dh}, could be set as zero if not taken into consideration [12]. The desired positions, x_{md} and x_{sd}, are given as follows:

$$x_{md} = \int_0^t (u_m + \hat{v}_m)/(\sqrt{2b})d\sigma \tag{22}$$

$$x_{sd} = \int_0^t (\hat{u}_s + v_m)/(\sqrt{2b})d\sigma \tag{23}$$

Moreover, x_{mf} and x_{sf} are the fictitious positions described as below

$$x_{mf}(t) = (\int_0^{t-T_1(t)} u_m d\sigma + \int_0^t v_s d\sigma)/(\sqrt{2b}) \tag{24}$$

$$x_{sf}(t) = (\int_0^t u_m d\sigma + \int_0^{t-T_2(t)} v_s d\sigma)/(\sqrt{2b}) \tag{25}$$

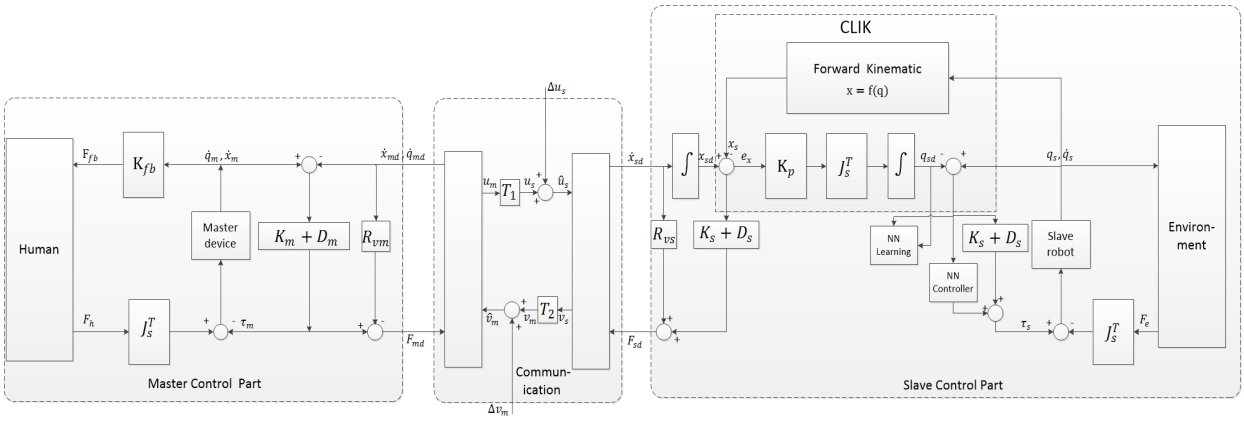

Fig. 7. Teleoperation control using the wave correction scheme with global neural controllers

From Eqs. (20) and (21), the corrective waves are proportional to the difference between the desired and fictitious positions, and the goals are to achieve

$$x_{sd}(t) - x_{md}(t - T_1(t)) \to \frac{1}{\sqrt{2b}} \int_{t-T_1(t)-T_2(t)}^{t} v_s d\sigma \to 0$$

$$x_{md}(t) - x_{sd}(t - T_2(t)) \to \frac{1}{\sqrt{2b}} \int_{t-T_1(t)-T_2(t)}^{t} u_m d\sigma \to 0$$

When the waves become zero, the desired position difference will converge to an ideal value [12], which will be particularly useful for trajectory and force control. After applying the correction method, in the next section the controller design and the stability analysis of the teleopration system will be discussed.

III. NEURAL CONTROL DESIGN BASED ON WAVE VARIABLE

A. Basic PD control design

In this section, a control scheme is proposed using a torque control based on the nominal model and a NN controller to deal with the uncertainties. The control system on both the master and the slave sides is first designed following basic PD control technique. Consider the dynamics models of the master device (3) and of the slave robot (6). The following controllers are introduce for them, respectively.

$$\tau_m = K_m e_m + D_m \dot{e}_m \tag{26}$$

$$\tau_s = -K_s e_s - D_s \dot{e}_s \tag{27}$$

where $e_i = q_i - q_{id}$ is the tracking error, $q_{id} \in \mathbb{R}^n$ is the desired joint angle served as the reference command for the local PD controller, $K \in \mathbb{R}^{n\times n}$ and $D \in \mathbb{R}^{n\times n}$ are the symmetric positive definite matrices for the joint angle and angular velocity gains. The subscript "i" stands for "m" and "s", which denote the master device and the slave robot, respectively.

Define the generalized tracking error

$$e_{vs} = \dot{e}_s + K_{s1} e_s \tag{28}$$

where $K_{s1} = D_s^{-1} K_s$.

$$\tau_s = -D_s e_{vs} \tag{29}$$

Define $q_v = \dot{q}_d - K_{s1} e_s$, and the dynamics of the slave (6) and (7) can be rewritten as

$$M_s \dot{e}_{vs} + C_s e_{vs} + G_s + M_s \dot{q}_v + C_s q_v = \tau_s - J_s^T F_e + f_s \tag{30}$$

By substituting (29) into (30), we have

$$M_s \dot{e}_{vs} + C_s e_{vs} + D_s e_{vs} = -J_s^T F_e + f_s - G_s + M_s \dot{q}_v - C_s q_v \tag{31}$$

and the uncertain nonlinear dynamics with the input z could be described by

$$F(z) = J_s^T F_e + f_s - G_s + M_s \dot{q}_v - C_s q_v \tag{32}$$

For trajectory tracking, if the dynamics of the robot is available, with appropriate selection of the angular position and angular velocity gains K and D, the PD control could guarantee the stability of the closed loop system. For uncertain models, the conventional PD controller may not be able to guarantee the global asymptotic stability [55]. As above mentioned, the NN is of powerful function approximation ability, which could be used for the identification of the uncertainties.

As indicated by Eq. (9), the model of the human operator could be regarded as an intelligent PI controller, which could adjust the output force and position in real time. In this work, we focus on the accurate position control of the slave telerobot.

B. Task Space Position-to-Position Control

In this paper, the CLIK method is employed for position-to-position control of the slave robot, which could avoid kinematic singularities and numerical drifts when solving inverse kinematics problem [3].

The desired slave joint velocity could be described in the CLIK algorithm as below

$$q_{sd} = \int K_p J_s^T(q) e d\sigma \tag{33}$$

where $e = x_{sd} - x_s$ is the error between the desired slave trajectory x_{sd} and the actual slave trajectory x_s, K_p is a positive definite matrix adjusting the convergence rate [56] and $J_s^T(q)$ is transpose of the Jacobian matrix. This method may avoid the problems occurring in open-loop form and the block diagram of the CLIK algorithm is given in Fig. 7.

C. RBF Neural Networks

RBF NN could be used to approximate the dynamics of the robotic model with its local generalization network. It could greatly accelerate the learning speed, avoid the local minimum problem and improve the tracking accuracy of the robot especially for those with complicated structures and large numbers of DOFs [57]. The RBF NNs could be expressed as below:

$$\varphi_i = exp(-\frac{\|z - c_i\|^2}{\sigma_i^2}), i = 1, 2, ..., n \tag{34}$$

$$\hat{F}(z) = \hat{W}^T \varphi(z) \tag{35}$$

where $z \in \mathbb{R}^n$ is the input vector and n represents the DOF of the slave robot, which is 7 for the left arm of the Baxter robot, $\hat{F}(z) \in \mathbb{R}^n$ is the output vector, $\varphi = [\varphi_1, \varphi_2, ..., \varphi_n]^T$ is the output vector of the hidden layer, $\hat{W} \in \mathbb{R}^{N \times n}$ is the weight matrix which connects the hidden layer and the output layer, and N represents the hidden nodes number, $c_i \in \mathbb{R}^n$ and $\sigma_i > 0$ are the center vector and width of the ith hidden node. From Eq. (34) the output of the hidden nodes in the RBF NNs are calculated by a radially symmetric function (e.g., Gaussian function).

The adjustable parameters in the RBF NNs (34) and (35) are the weight matrix $\hat{W}$, the center vector c_i and the width σ_i of every hidden node. Usually, the values of c_i and σ_i are chosen according to the knowledge of the system or by pretreatment training. The output of the network $\hat{F}(z)$ is linear with respect to weight matrix $\hat{W}$, which greatly simplifies the analysis and learning process of the RBF NNs.

In this paper, the RBF NNs are employed to approximate the uncertain nonlinear function $F(z)$ [57], [58], and the following lemmas are given.

Lemma 1: The input vector of RBF NNs $z \in X$, where X is a compact subset.

Lemma 2: Given a positive constant ε_0 and a continuous function $F : z \to \mathbb{R}^n$, there exists a weight matrix $W^* \in \mathbb{R}^{N \times n}$, making the output of a RBF NN with N hidden nodes $\hat{F}(z)$ satisfy

$$\max_{z \in X} \|\hat{F}(z, W^*) - F(z)\| \leqslant \varepsilon \tag{36}$$

where N is determined by the precision parameter ε_0 and the function $F(z)$. $\hat{F}(z, W^*)$ is the estimate of the output $F(z)$ with the ideal weight matrix W^*.

Lemma 3: The output of a RBF NN $\hat{F}(z, \hat{W})$ on its arguments $z, \hat{W}$ is continuous.

Therefore, (30) could be rewritten as follows

$$M_s \dot{e}_{vs} = -(C_s + D_s) e_{vs} + \hat{F}(z, W^*) + \eta \tag{37}$$

where $\eta = F(z) - \hat{F}(z, W^*)$ and W^* is the optimal weight matrix corresponding to $z \in X$, i.e.

$$\|F(z) - \hat{F}(z, W^*)\| = \min \sup_{z \in X} \|F(z) - \hat{F}(z, \hat{W})\| \tag{38}$$

where η is bounded by $\eta_0 := \sup_{z \in X} \|F(z) - \hat{F}(z, W^*)\|$.

According to the properties of the RBF NN, (36) could be rewritten as

$$M_s \dot{e}_{vs} = -(C_s + D_s) e_{vs} + W^{*T} \varphi(z) \tag{39}$$

With Lyapunov method it is easy to obtain the following update law

$$\dot{\hat{W}} = -Q^{-1} \varphi(z) e_{vs}^T \tag{40}$$

where Q is a symmetric positive definite matrix.

D. Controller Design

From (31) and (32), when $F(z) \neq 0_{m \times n}$, i.e., there exist uncertainties in the robot model, and the PD controller (27) could ensure the boundedness of the tracking error, but may not make it convergent to zero. Therefore, the RBF NN control is developed based on Lemmas 1−3.

The control torque is composed of two parts, as below

$$\tau_s = \tau_{PD} + \tau_{NN} \tag{41}$$

where τ_{PD} is the basic PD control and according to (27) and (29)

$$\tau_{PD} = -K_s e_s - D_s \dot{e}_s = -D_s e_{vs} \tag{42}$$

while τ_{NN} is the NN compensation controller

$$\tau_{NN} = \hat{F}(z) = \hat{W}^T \varphi(z) \tag{43}$$

Then the closed-loop system dynamics of the slave robot can be written as

$$M_s \dot{e}_{vs} + C_s e_{vs} + D_s e_{vs} = F_z - \hat{F}_z \tag{44}$$

E. Theoretical Analysis

(I) Convergence of the tracking error

Proof: Choose a candidate of Lyapunov function as follows

$$V_1 = \frac{1}{2} e_{vs}^T M_s e_{vs} + \frac{1}{2} tr(\widetilde{W}^T Q \widetilde{W}) \tag{45}$$

Then, we have

$$\begin{aligned}\dot{V}_1 =&\frac{1}{2}e_{vs}^T\dot{M}_s e_{vs} + e_{vs}^T M_s \dot{e}_{vs} + tr(\widetilde{W}^T Q\dot{\hat{W}})\\ =&\frac{1}{2}e_{vs}^T\dot{M}_s e_{vs} - e_{vs}^T C_s e_{vs} - e_{vs}^T D_s e_{vs}\\ &- tr[\widetilde{W}^T(\varphi(z)e_{vs}^T - QQ^{-1}\varphi(z)e_{vs}^T)]\\ =&- e_{vs}^T D_s e_{vs} < 0\end{aligned} \tag{46}$$

And we have

$$\int_0^t \dot{V}_1 d\sigma = V_1(t) - V_1(0) = \int_0^t (-e_{vs}^T D_s e_{vs}) d\sigma < 0 \tag{47}$$

such that we see $\dot{V}_1$ is strictly negative definite. According to [59], $e_{vs} \in L_2 \bigcap L_\infty$, $\dot{e}_{vs} \in L_\infty$, thus when $t \to \infty$, e_{vs} converges to zero asymptotically.

Then we choose the value of K_{s1} satisfying $\Re[\lambda_i(-K_{s1})] < 0$, $\forall i$, such that when $t \to \infty$, e_s and $\dot{e}_s$ converge to zero asymptotically and the detailed analysis could be found in [59].

(II) Stability of the teleoperation system

The proper selection of R_{vm} and R_{vs} that satisfy

$$\lambda_m(R_{vm}(t)) \geqslant \left(|\hat{v}_m|^2 - (1-\dot{T}_2)|v_m|^2\right)/2|\dot{x}_{md}|^2 \tag{48}$$

$$\lambda_m(R_{vs}(t)) \geqslant \left(|\hat{u}_s|^2 - (1-\dot{T}_1)|u_s|^2\right)/2|\dot{x}_{sd}|^2 \tag{49}$$

could guarantee the stability of the overall teleoperation system.

Proof: We choose another Lyapunov function candidate as below

$$V = V_c + V_w \tag{50}$$

where

$$V_w = \frac{1}{2}\int_{t-T_1}^t u_m^T u_m d\sigma + \frac{1}{2}\int_{t-T_2}^t v_s^T v_s d\sigma \tag{51}$$

$$\begin{aligned}V_c =&\frac{1}{2}\dot{q}_m^T M_m \dot{q}_m + \frac{1}{2}e_m^T K_m e_m + \frac{1}{2}e_{vs}^T M_s e_{vs}\\ &+ \frac{1}{2}tr(\widetilde{W}^T Q\widetilde{W})\end{aligned} \tag{52}$$

According to [12], we have

$$\begin{aligned}\dot{V}_w =&\frac{1}{2}(\dot{T}_1|u_s|^2 + |\delta u_s|^2 + 2u_s^T\delta u_s + \dot{T}_2|v_m|^2\\ &+ |\delta v_m|^2 + 2v_m^T\delta v_m)\end{aligned} \tag{53}$$

Considering (47) and (48), we have

$$\dot{V}_w \leqslant -\dot{x}_{md}^T R_{vm}^{'}\dot{x}_{md} - \dot{x}_{sd}^T R_{vs}^{'}\dot{x}_{sd} \tag{54}$$

where $R_{vm}^{'} = R_{vm} - \lambda(R_{vm})I$ and $R_{vs}^{'} = R_{vs} - \lambda(R_{vs})I$.

As for the controllers on both the master and the slave sides, assume that the operator and the environment are passive [12] and could be written as

$$\begin{aligned}\int_0^t \dot{x}_m^T(-F_h)d\sigma \geqslant V_h(t) - V_h(0)\\ \int_0^t \dot{x}_s^T F_e d\sigma \geqslant V_e(t) - V_e(0)\end{aligned} \tag{55}$$

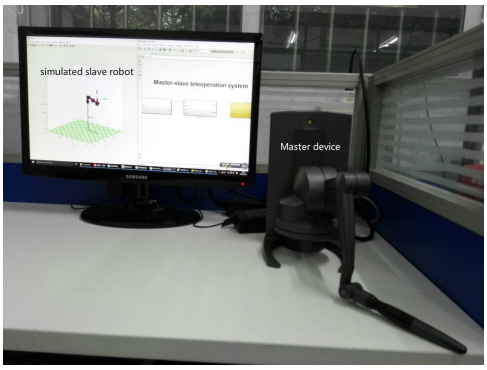

Fig. 8. The experiment platform of the master-slave teleoperation system [photo take at South China University of Technology].

where V_h and V_e stand for the bounded storage functions. And according to (45), then we have

$$\dot{V}_c = \dot{x}_m^T F_h - \dot{x}_s^T F_e - \dot{q}_m^T D_m \dot{q}_m + \dot{V}_1 \tag{56}$$

Considering Eqs. (47), (54) and (55), finally we could obtain

$$\begin{aligned}V(t) - V(0) \leqslant &\int_0^t (\dot{x}_m^T F_h - \dot{x}_s^T F_e)\\ &- \int_0^t \left(\dot{x}_{md}^T R_{vm}^{'}\dot{x}_{md} + \dot{x}_{sd}^T R_{vs}^{'}\dot{x}_{sd}\right) d\sigma\\ &+ \int_0^t \left(\dot{V}_1 - \dot{q}_m^T D_m \dot{q}_m\right) d\sigma\end{aligned} \tag{57}$$

which guarantees boundedness of V under the condition of passivity of the teleoperation system.

IV. EXPERIMENTS

The comparative experiments are performed for the following purposes: i) to show that the RBF NN compensation is effective to improve the tracking performance, in comparison with typical PD control without compensation; ii) to demonstrate that the wave variable technique enhanced master-slave teleoperation system remains stable in the presence of various time delays; and iii) to illustrate the seamless combination of neural control scheme and wave variable technique for teleoperation system.

A. Experiment Platform

The experimental platform is set up with the TouchX haptic device and a computer connected to it, as well as the slave robot Baxter simulated using MATLAB Robotics Toolbox (see Figs. 8 and 9). The human operator moves the stylus of the TouchX joystick, through which the desired trajectory is sent to the simulated communication channels and the contact force between the simulated robot and the environment is regulated. Through the communication channels, the desired position of the slave robot is passed to the simulated left arm of the Baxter robot.

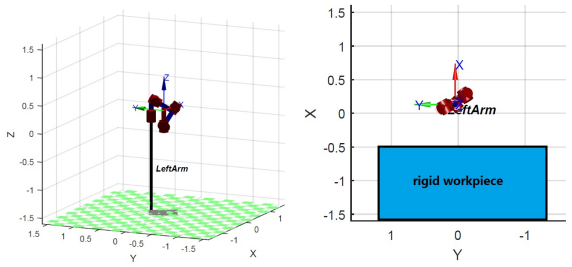

Fig. 9. The simulated slave robot.

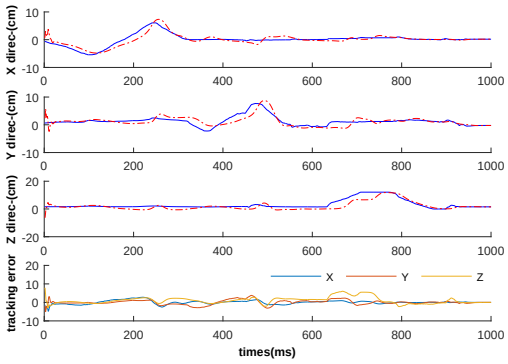

Fig. 10. The trajectory of the master device (solid) and the slave (dashed) with the conventional PD controller.

B. Trajectory Tracking under Different Controllers

First the controller for the slave robot is designed as a typical PD controller. A desired trajectory set by the master device (TouchX) for the slave robot (simulated Baxter robot arm) is designed, which requires the human operator to move the stylus of the master joystick from an initial position to the minimum value along the X direction, then to the maximum value along the X direction and finally restore back to the initial position, for a time span of $0 \sim 3$s. Then, the human operator performs the same motion along the Y direction for $3 \sim 6$s, and along the Z direction for $6 \sim 9$s. The trajectory tracking result for the slave robot with the conventional PD controller is shown in Fig. 10.

Then, the RBF NN control is added on top of the basic PD controller to compensate for the uncertain nonlinear dynamics. In this experiment, the first 10s is reserved for NN training. It is clear that the weights for different joints converge to different values, among which the values of the normed weights for joints $S1$, $W0$ and $W2$ are close to 0, for they are almost not affected by gravity during the movement of the robot. At $10 \sim 19$s the human operator repeats the process of the last experiment. The weights of the NN are shown in Fig. 11. In comparison to the tracking performance of two experiments shown in Figs. 10 and 12, after adding the RBF NN controller, the tracking performance of the slave robot is much improved.

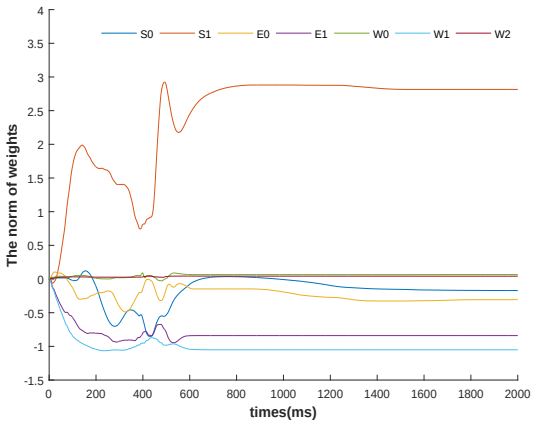

Fig. 11. The norm of NN weights for each joint of the slave robot during NN training.

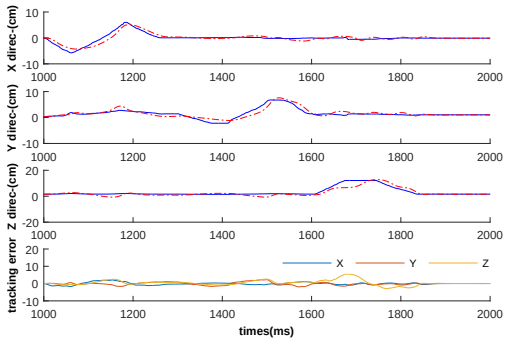

Fig. 12. The trajectory of the master device (solid) and the slave (dashed) with the RBF NN compensation.

C. Trajectory and Force Reflection under Different Communications

Under the circumstances of time-varying delays, the system is very likely to become unstable and uncontrollable. In this section, we test the wave variables technique in the communication of the teleoperation system, and then perform compar-

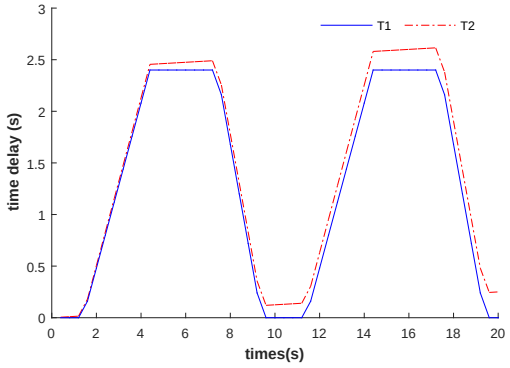

Fig. 13. Varying time delays T_1 (solid) and T_2 (dashed).

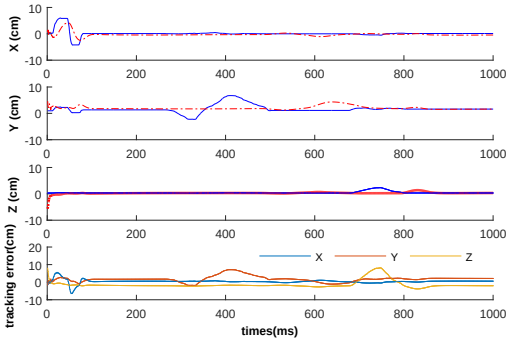

Fig. 14. The trajectory of the master device (solid) and the slave (dashed) with time-varying delayed communication, using wave variable technique.

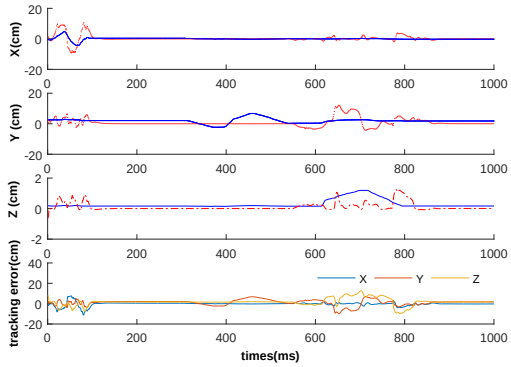

Fig. 15. The trajectory of the master device (solid) and the slave (dashed) with time-varying delayed communication, without using the wave variable technique.

ison with the other set of experiment without using the wave variables. The added time delays T_1 and T_2 in the experiment are illustrated in Fig. 13, and the force reflection to the human operator in Fig. 7 is calculated by $F_{fb} = K_{fb}(x_s - x_m)$.

The human operator is required to repeat the movement twice of the last experiment, one with wave variables in the communication channels and the other without. The trajectory tracking performances of the two comparative experiments are shown in Figs. 14 and 15. In the force reflection experiment, a rigid workpiece similar to a wall is set up and installed along the X direction, as shown in Fig. 9. In the first 3 seconds both the master device and the slave robot are in free motion. Then the master begins to move towards the place where the slave will get in touch with the workpiece and the contact will last for about 10s. During the contact with the workpiece, the slave robot almost does not move, and the environmental force applied on the slave robot converges to a set value, and the operator holds the master device with a constant force. Then, the operator moves the master joystick back in free motion, and the slave robot leaves the workpiece and tracks the master's motion without the time-varying delays. The trajectories along the X direction of the master device

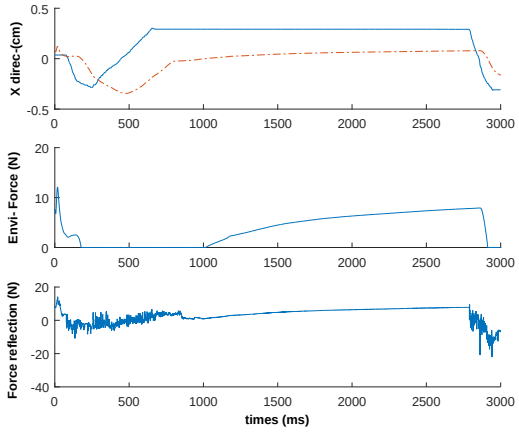

Fig. 16. (1) Top: the trajectories along the X direction of the master device (solid) and of the slave (dashed) with time-varying delayed communication, using wave variable technique. (2) Middle: the environmental force to the slave robot. (3) Bottom: the force reflections to the master device along the X direction with time-varying delayed communication, using wave variable technique.

and of the slave telerobot and the force reflections with time-varying delays and the wave variables are shown in Fig. 16. The oscillation as can be seen is due to the process of force feedback before and after the contact.

V. Conclusions

In this paper, a teleoperation control method has been investigated in the presence of time-varying delays and uncertain robot dynamics. The RBF NN and wave variable technique are effectively combined to solve the problems caused by uncertainties and time delays. Rigorous theoretical analysis has been performed to establish passive property and stability of the teleoperation system. Comparative experiments have been carried out to validate the proposed method. Studies of teleopeation in an unknown environment will be conducted in the future work.

References

[1] "Geomagic touchx haptic device," http://www.geomagic.com/en/products/phantom-desktop/overview.

[2] L. Hu and G. Liu, "The wave-variable teleoperator with improved trajectory tracking," in *International Conference on Control and Automation*, 2010, pp. 322–327.

[3] C. Yang, H. Ma, and M. Fu, *Advanced Technologies in Modern Robotic Applications*. Springer, Singapore, 2016.

[4] P. Corke, "Robotics, vision and control," *Springer Tracts in Advanced Robotics*, vol. 73, no. 6, 2011.

[5] M. Wu, Y. He, J. H. She, and G. P. Liu, "Delay-dependent criteria for robust stability of time-varying delay systems," *Automatica*, vol. 40, no. 8, pp. 1435–1439, 2004.

[6] J. P. Richard, "Time-delay systems: an overview of some recent advances and open problems," *Automatica*, vol. 39, no. 10, pp. 1667–1694, 2003.

[7] R. J. Anderson and M. W. Spong, "Bilateral control of teleoperators with time delay," *IEEE Transactions on Automatic Control*, vol. 34, no. 5, pp. 494–501, 1989.

[8] X. Yang, C. Hua, J. Yan, and X. Guan, "An exact stability condition for bilateral teleoperation with delayed communication channel," *IEEE Transactions on Systems Man & Cybernetics: Systems*, vol. 46, no. 3, pp. 434–439, 2016.

[9] J.-J. E. Slotine and W. Li, "Applied nonlinear control," *Applied Nonlinear Control*, 1991.

[10] Y. Gu, C. Zhang, and K. T. Chong, "Adaptive passive control with varying time delay," *Simulation Modelling Practice & Theory*, vol. 18, no. 1, pp. 1–8, 2010.

[11] M. Satler, C. A. Avizzano, A. Frisoli, P. Tripicchio, and M. Bergamasco, "Bilateral teleoperation under time-varying delay using wave variables," in *IEEE/RSJ International Conference on Intelligent Robots and Systems*, 2009, pp. 4596–4602.

[12] P. Pitakwatchara, "Control of time-varying delayed teleoperation system using corrective wave variables," in *Proceedings of the IEEE/RSJ International Conference on Intelligent Robots and Systems(IROS)*. Hamburg: IROS, Sept.28- Oct.2 2015.

[13] F. Hong, S. S. Ge, B. Ren, and T. H. Lee, "Robust adaptive control for a class of uncertain strict-feedback nonlinear systems," *International Journal of Robust & Nonlinear Control*, vol. 19, no. 7, pp. 746–767, 2009.

[14] M. Chen, S. S. Ge, and B. Ren, "Adaptive tracking control of uncertain mimo nonlinear systems with input constraints." *Automatica*, vol. 47, no. 3, pp. 452–465, 2011.

[15] W. He, S. Zhang, and S. S. Ge, "Adaptive control of a flexible crane system with the boundary output constraint," *IEEE Transactions on Industrial Electronics*, vol. 61, no. 8, pp. 4126–4133, 2014.

[16] W. He, W. Ge, Y. Li, Y. J. Liu, C. Yang, and C. Sun, "Model identification and control design for a humanoid robot," *IEEE Transactions on Systems Man & Cybernetics: Systems*, 2016.

[17] D. Zhai and Y. Xia, "Adaptive fuzzy control of multilateral asymmetric teleoperation for coordinated multiple mobile manipulators," *IEEE Transactions on Fuzzy Systems*, vol. 24, no. 1, pp. 57–70, 2016.

[18] W. He and S. S. Ge, "Cooperative control of a nonuniform gantry crane with constrained tension," *Automatica*, vol. 66, pp. 146–154, 2016.

[19] D. H. Zhai and Y. Xia, "Adaptive control of semi-autonomous teleoperation system with asymmetric time-varying delays and input uncertainties." *IEEE Transactions on Cybernetics*, 2016.

[20] ——, "Adaptive control for teleoperation system with varying time-delays and input saturation constraints," *IEEE Transactions on Industrial Electronics*, 2016.

[21] Y. Li, S. Tong, and T. Li, "Adaptive fuzzy output feedback dynamic surface control of interconnected nonlinear pure-feedback systems," *IEEE Transactions on Cybernetics*, vol. 45, no. 1, pp. 138–149, Jan 2015.

[22] Y. Li, S. Sui, and S. Tong, "Adaptive fuzzy control design for stochastic nonlinear switched systems with arbitrary switchings and unmodeled dynamics," *IEEE Transactions on Cybernetics*, 2016.

[23] Y. Li and S. Tong, "Adaptive fuzzy output-feedback stabilization control for a class of switched nonstrict-feedback nonlinear systems," *IEEE Transactions on Cybernetics*, vol. PP, no. 99, pp. 1–10, 2016.

[24] Y. Gao and Y. J. Liu, "Adaptive fuzzy optimal control using direct heuristic dynamic programming for chaotic discrete-time system," *Journal of Vibration & Control*, vol. 22, no. 2, pp. 595–603, 2014.

[25] Y. J. Liu and S. Tong, "Adaptive fuzzy control for a class of nonlinear discrete-time systems with backlash," *IEEE Transactions on Fuzzy Systems*, vol. 22, no. 5, pp. 1359–1365, Oct 2014.

[26] X. W. Chen, J. G. Zhang, and Y. J. Liu, "Research on the intelligent control and simulation of automobile cruise system based on fuzzy system," *Mathematical Problems in Engineering*, vol. 2016, no. 5, pp. 1–12, 2016.

[27] C. Sun, W. He, W. Ge, and C. Chang, "Adaptive neural network control of biped robots," *IEEE Transactions on Systems Man & Cybernetics: Systems*, pp. 1–12, 2016.

[28] C. Yang, Z. Li, R. Cui, and B. Xu, "Neural network-based motion control of an underactuated wheeled inverted pendulum model," *IEEE Transactions on Neural Networks and Learning Systems*, vol. 25, no. 11, pp. 2004–2016, 2014.

[29] G. X. Wen, C. L. P. Chen, Y. J. Liu, and Z. Liu, "Neural-network-based adaptive leader-following consensus control for second-order non-linear multi-agent systems," *IET Control Theory Applications*, vol. 9, no. 13, pp. 1927–1934, 2015.

[30] C. Yang, X. Wang, L. Cheng, and H. Ma, "Neural-learning-based telerobot control with guaranteed performance." *IEEE Transactions on Cybernetics*, pp. 1–12, 2016.

[31] Y. Hu, Z. Li, G. Li, P. Yuan, C. Yang, and R. Song, "Development of sensory-motor fusion-based manipulation and grasping control for a robotic hand-eye system," *IEEE Transactions on Systems Man & Cybernetics: Systems*, 2016.

[32] L. Cheng, Z. G. Hou, M. Tan, Y. Lin, and W. Zhang, "Neural-network-based adaptive leader-following control for multiagent systems with uncertainties," *IEEE Transactions on Neural Networks*, vol. 21, no. 8, pp. 1351–8, 2010.

[33] C. Yang, Y. Jiang, Z. Li, W. He, and C. Y. Su, "Neural control of bimanual robots with guaranteed global stability and motion precision," *IEEE Transactions on Industrial Informatics*, 2016.

[34] Z. Li, H. Xiao, C. Yang, and Y. Zhao, "Model predictive control of nonholonomic chained systems using general projection neural networks optimization," *IEEE Transactions on Systems Man & Cybernetics: Systems*, vol. 45, no. 10, pp. 1313–1321, 2015.

[35] W. He, Y. Chen, and Z. Yin, "Adaptive neural network control of an uncertain robot with full-state constraints," *IEEE Transactions on Cybernetics*, vol. 46, no. 3, pp. 620–629, 2016.

[36] Y. J. Liu and S. Tong, "Adaptive nn tracking control of uncertain nonlinear discrete-time systems with nonaffine dead-zone input." *IEEE Transactions on Cybernetics*, vol. 45, no. 3, pp. 497–505, 2015.

[37] W. He, A. O. David, Z. Yin, and C. Sun, "Neural network control of a robotic manipulator with input deadzone and output constraint," *IEEE Transactions on Systems Man & Cybernetics: Systems*, vol. 46, no. 6, pp. 759–770, 2016.

[38] W. He, Z. Yin, and C. Sun, "Adaptive neural network control of a marine vessel with constraints using the asymmetric barrier lyapunov function." *IEEE Transactions on Cybernetics*, pp. 1–11, 2016.

[39] Z. Liu, C. Chen, Y. Zhang, and C. L. Chen, "Adaptive neural control for dual-arm coordination of humanoid robot with unknown nonlinearities in output mechanism." *IEEE Transactions on Cybernetics*, vol. 45, no. 3, pp. 521–532, 2014.

[40] Y. J. Liu, L. Tang, S. Tong, and C. L. Chen, "Adaptive nn controller design for a class of nonlinear mimo discrete-time systems." *IEEE Transactions on Neural Network and Learning Systems*, vol. 26, no. 5, pp. 1007 – 1018, 2015.

[41] Y. J. Liu, S. Tong, C. L. P. Chen, and D. J. Li, "Neural controller design-based adaptive control for nonlinear mimo systems with unknown hysteresis inputs," *IEEE Transactions on Cybernetics*, vol. 46, no. 1, pp. 9–19, 2016.

[42] Y. Lu, J. K. Liu, and F. C. Sun, "Actuator nonlinearities compensation using RBF neural networks in robot control system," in *IMACS Multiconference on Computational Engineering in Systems Applications*, 2006, pp. 231–238.

[43] J. Li and T. Duckett, "Some practical aspects on incremental training of RBF network for robot behavior learning," in *actuator nonlinearitiesWorld Congress on Intelligent Control and Automation*, 2008, pp. 2001 – 2006.

[44] J. Liu and Y. Lu, "Adaptive RBF neural network control of robot with actuator nonlinearities," *Journal of Control Theory & Applications*, vol. 08, no. 2, pp. 249–256, 2010.

[45] L. Xue, W. Fan, and X. Wang, "Research on motion trajectory control of fruit and vegetable picking robot based on RBF network," *Journal of Agricultural Mechanization Research*, 2016.

[46] C. H. Tsai and H. T. Chuang, "Deadzone compensation based on constrained RBF neural network," *Journal of the Franklin Institute*, vol. 341, no. 4, pp. 361–374, 2004.

[47] F. G. Rossomando, C. Soria, and R. Carelli, "Autonomous mobile robots navigation using RBF neural compensator," *Control Engineering Practice*, vol. 19, no. 3, pp. 215–222, 2011.

[48] X. Wang, C. Yang, and Z. Li, "Development of a touchx based teleoperation approach using wave variable technique," in *Proceedings of the IEEE International Conference on Advanced Robotics and Mechatronics (ICARM), in press*. Macau: ICARM, 2016.

[49] J. J. Craig, *Adaptive control of mechanical manipulators*. Addison-Wesley, 1986.
[50] C. S. G. Lee, R. C. Gonzalez, and K. S. Fu, "Tutorial on robotics," *IEEE Computer Society Los Alamitos Ca*, 1983.
[51] R. N. Murray, Z. Li, S. Sastry, R. N. Murray, Z. Li, and S. Sastry, *A mathematical introduction to robotics manipulation.*, 1994.
[52] C. Yang, X. Wang, L. Cheng, and H. Ma, "Neural-learning-based telerobot control with guaranteed performance," *IEEE Transactions on Cybernetics*, vol. PP, no. 99, pp. 1–12, 2016.
[53] D. A. Lawrence, "Stability and transparency in bilateral teleoperation," *IEEE Transactions on Robotics & Automation*, vol. 9, no. 5, pp. 624–637, 1993.
[54] D. H. Zhai and Y. Xia, "Adaptive finite-time control for nonlinear teleoperation systems with asymmetric time-varying delays," *International Journal of Robust & Nonlinear Control*, pp. 2586–2607, 2016.
[55] R. Kelly, "Global positioning of robot manipulators via PD control plus a class of nonlinear integral actions," *IEEE Transactions on Automatic Control*, vol. 43, no. 7, pp. 934–938, 1998.
[56] L. Sciavicco and B. Siciliano, "A dynamic solution to the inverse kinematic problem for redundant manipulators," in *IEEE International Conference on Robotics and Automation*, 1987, pp. 1081–1087.
[57] J. Park and I. Sandberg, "Universal approximation using radial-basis-function networks," *Neural Computation*, vol. 3, no. 2, pp. 246–257, 1991.
[58] D. H. Zhai and Y. Xia, "Adaptive stabilization of nonlinear teleoperation systems: An SIIOS approach," *International Journal of Robust & Nonlinear Control*, pp. 1–13, 2016.
[59] Q. Zhou, J. Xu, and T. P. Leung, "Globally stable adaptive controller of robot manipulators," in *IEEE Region 10 Conference on Computer, Communication, Control and Power Engineering*, vol. 4, 1993, pp. 90–93.

Chenguang Yang (M'10-SM'16) received the B.Eng. degree in measurement and control from Northwestern Polytechnical University, Xi'an, China, in 2005, and the Ph.D. degree in control engineering from the National University of Singapore, Singapore, in 2010. He received postdoctoral training at Imperial College London, UK. He is a senior lecturer with Zienkiewicz Centre for Computational Engineering, Swansea University, UK. He is also with South China Univeristy of Technology, China. His research interests lie in robotics, automation and computational intelligence.

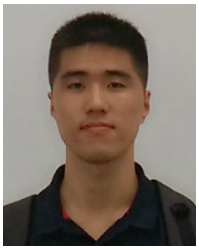

Xingjian Wang received the B.E. degree in automation from South China University of Technology, Guangzhou, China, in 2015, and is currently working toward the M.S. degree at the South China University of Technology, Guangzhou, China. His research interests include robotics and teleoperation control.

Zhijun Li (M'07-SM'09) received the Ph.D. degree in mechatronics, Shanghai Jiao Tong University, P. R. China, in 2002. From 2003 to 2005, he was a postdoctoral fellow in Department of Mechanical Engineering and Intelligent systems, The University of Electro-Communications, Tokyo, Japan. From 2005 to 2006, he was a research fellow in the Department of Electrical and Computer Engineering, National University of Singapore, and Nanyang Technological University, Singapore. From 2007-2011, he was an Associate Professor in the Department of Automation, Shanghai Jiao Tong University, P. R. China. In 2008, he was a visiting scholar in Microsoft Research Asia, Beijing. Since 2012, he is a Professor in College of Automation Science and Engineering, South China university of Technology, Guangzhou, China. In 2015, he is a visiting professor in Faculty Science and Technology, the University of Macau, Macau, China, and Department of Advanced Robotics, Italian Institute of Technology, Genoa, Italy. From 2016, he is the Chair of Technical Committee on Biomechatronics and Biorobotics Systems (B2S), IEEE Systems, Man and Cybernetics Society. He is serving as an Editor-at-large of Journal of Intelligent & Robotic Systems, Associate Editors of IEEE Transactions on Neural Networks and Learning Systems and IEEE Transactions on Systems, Man and Cybernetics: Systems, and IEEE Transactions on Automation Science and Engineering. He has been the General Chair of 2016 IEEE Conference on Advanced Robotics and Mechatronics, Macau, China. Dr. Li's current research interests include service robotics, tele-operation systems, nonlinear control, neural network optimization, etc.

Yanan Li (S'10-M'14) received the BEng and MEng degrees from the Harbin Institute of Technology, China, in 2006 and 2008, respectively, and the Ph.D. degree from the NUS Graduate School for Integrative Sciences and Engineering, National University of Singapore, in 2013. He has been a Research Scientist with the I2R, A*STAR, from 2013 to 2015. He is currently a Research Associate with the Department of Bioengineering, Imperial College London, UK. His research interests include physical human-robot interaction and robot control.

Chun-Yi Su (SM'99) received the Ph.D. degree in control engineering from the South China University of Technology, Guangzhou, China, in 1990. He joined Concordia University, Montreal, QC, Canada, in 1998, after a seven-year stint with the University of Victoria, Victoria, BC, Canada. He is currently with the College of Automation Science and Engineering, South China University of Technology, on leave from Concordia University. His current research interests include the application of automatic control theory to mechanical systems. He is particularly interested in control of systems involving hysteresis nonlinearities. He has authored or co-authored over 300 publications in journals, book chapters, and conference proceedings. Dr. Su has served as an Associate Editor of the IEEE TRANSACTIONS ON AUTOMATIC CONTROL, the IEEE TRANSACTIONS ON CONTROL SYSTEMS TECHNOLOGY, and the Journal of Control Theory and Applications. He has been on the Editorial Board of 18 journals, including the IFAC Journal of Control Engineering Practice and Mechatronics.